CHEMISTRY

Stretching vibration is a spectator in nucleophilic substitution

Martin Stei[1]*, Eduardo Carrascosa[1†], Alexander Dörfler[1], Jennifer Meyer[1], Balázs Olasz[2], Gábor Czakó[2], Anyang Li[3], Hua Guo[4], Roland Wester[1‡]

How chemical reactions are influenced by reactant vibrational excitation is a long-standing question at the core of chemical reaction dynamics. In reactions of polyatomic molecules, where the Polanyi rules are not directly applicable, certain vibrational modes can act as spectators. In nucleophilic substitution reactions, CH stretching vibrations have been considered to be such spectators. While this picture has been challenged by some theoretical studies, experimental insight has been lacking. We show that the nucleophilic substitution reaction of F^- with CH_3I is minimally influenced by an excitation of the symmetric CH stretching vibration. This contrasts with the strong vibrational enhancement of the proton transfer reaction measured in parallel. The spectator behavior of the stretching mode is supported by both quasi-classical trajectory simulations and the Sudden Vector Projection model.

INTRODUCTION

How reactant vibrational excitation affects chemical reactions is a long-standing subject of research. For atom-diatom collisions, Polanyi (*1*) already rationalized decades ago the first rules linking the influence of vibration to the position of the transition state on the potential energy surface (PES). For systems containing more than three atoms, this question becomes more complicated due to the presence of different vibrational modes and more complex transition-state geometries. Gas-phase studies on neutral-neutral reactions (*2*, *3*) find various forms of influence, which include rate decrease (*4*), as well as rate enhancement (*5*) and the opening of scattering resonances (*6*). Liu *et al.* (*7*) have recently discussed whether rate enhancement can, in some cases, be considered a rotational effect. Excitation of vibrational motion also affects surface reactions (*8*, *9*), and vibrational mode specificity has been found in ion-molecule reactions, which had been considered to evolve statistically (*10*). In some reactions, the polarization of the excitation laser can exert active steric control (*11*). Jiang and Guo (*12*) proposed the Sudden Vector Projection (SVP) model to generalize Polanyi's rules for more complex systems. This model treats the reaction within the sudden limit and attributes the enhancement of reactivity by a reactant mode to the projection of its normal mode vector onto the reaction coordinate at the transition state.

Reactions of the type $X^- + R\text{-}Y \rightarrow X\text{-}R + Y^-$ are widely studied as they represent model systems for bimolecular nucleophilic substitution (S_N2) reactions (*13*). In the gas phase, S_N2 reactions are often characterized by a double-well PES, which stems from the intermediate ion-dipole complexes in the entrance and exit channels on either side of the central barrier (*14*). In addition, hydrogen-bonded complexes have been found for small negative ions (*15*). For many exothermic reactions, the central barrier lies below the energy of reactants. Nevertheless, it has a substantial influence on the reaction kinetics by introducing dynamical constraints with respect to angular momentum, intramolecular energy transfer, or steric bottlenecks (*16*). Conventionally, these reactions have been treated statistically, assuming energy randomization in the intermediate complexes. While this is usually valid for large molecules, it is known that S_N2 reactions of smaller systems, for example, halide or hydroxyl anions with methyl halides, show nonstatistical behavior and the full dynamics need to be considered for their appropriate description (*17*, *18*). A wealth of atomistic reaction mechanisms could be identified by comparing experimental velocity and angle differential cross sections with quasi-classical trajectory (QCT) calculations (*19*, *20*). The branching ratio into these mechanisms is influenced not only by the shape of the PES but also by dynamical effects (*21*).

Because of the textbook colinear approach, methyl CH symmetric stretching vibrations have often been considered spectators for nucleophilic substitution, while CY vibrations are expected to enhance the reaction rate. However, Mikosch *et al.* (*22*) found that the colinear C_{3v}-symmetric approach is not always followed. Measurements of reaction rate constants for S_N2 reactions at different temperatures supported the spectator mode picture for statistically excited ensembles (*17*). Early foundational work on trajectory simulations has shown that mode-selective vibrational excitation may enhance the reactivity of S_N2 reactions (*23*, *24*). Previous works (*25*, *26*) found indirect evidence on the role of specific vibrations by exciting vibrations of the entrance channel complexes. These findings have been supported by QCT calculations (*15*) but challenged by quantum dynamical calculations (*27*). The latter predict an influence of all symmetric vibrational modes on the reaction rate of Cl^- with CH_3Br. Recent quantum wavepacket dynamics simulations predict a change from rate enhancement to rate reduction with increasing collision energy upon excitation of the CY bond (*28*). In these studies, the CH_3 umbrella mode has been found to have little influence. Recent trajectory calculations predict a small rate enhancement for the F^- + CH_3Cl S_N2 reaction by CH stretching vibrations (*29*, *30*), while quantum dynamics calculations predict inhibition upon CH stretching excitation, but all these results show strong collision energy dependence. Clear predictions are also hampered by the fact that full-dimensional

[1]Institut für Ionenphysik und Angewandte Physik, Universität Innsbruck, Technikerstraße 25/3, 6020 Innsbruck, Austria. [2]Department of Physical Chemistry and Materials Science, University of Szeged, Rerrich Béla tér 1, Szeged H-6720, Hungary. [3]Key Laboratory of Synthetic and Natural Functional Molecule Chemistry, Ministry of Education, College of Chemistry and Materials Science, Northwest University, 710127 Xian, P. R. China. [4]Department of Chemistry and Chemical Biology, University of New Mexico, Albuquerque, NM 87131, USA.
*Present address: Swarovski Technology, D. Swarovski KG, Swarovskistraße 30, 6112 Wattens, Austria.
†Present address: School of Chemistry, University of Melbourne, Parkville, Victoria 3010, Australia.
‡Corresponding author. Email: roland.wester@uibk.ac.at

calculations can only be performed classically, while quantum calculations are limited to at most six of the at least 12 dimensions of the inter- and intramolecular dynamics.

Here, we directly address the question of spectator mode dynamics experimentally. We probe whether the symmetric CH stretching vibration in CH_3I is a spectator mode during the S_N2 reaction with F^-. For this, we make use of the proton transfer reaction, which may also occur between the same reactants and leads to a deprotonated methyl iodide, CH_2I^-, product ion (*31*)

$$F^- + CH_3I \rightarrow CH_3F + I^- \ \Delta H = -1.96 \text{ eV} \quad (S_N2) \qquad (1)$$

$$\rightarrow HF + CH_2I^- \ \Delta H = +0.69 \text{ eV} \quad (\text{Proton transfer}) \qquad (2)$$

In contrast to the S_N2 reaction, which is exoergic and shows a high reaction rate coefficient up to 1 eV of collision energy (*32*), the proton transfer reaction is endoergic [see Fig. 1 for the stationary points along the reaction coordinate taken from (*33*)]. Both reaction channels feature the same prereaction complex, which is characterized by a hydrogen bond between the nucleophile F^- and a hydrogen atom of the methyl moiety (see Fig. 1). The energy profile of the proton transfer channel is rather flat once the initial barrier is overcome. Three closely lying transition states are found in which the HF is already preformed. One can expect vibrational excitation to promote the proton transfer reaction (*34*). Consequently, by studying both reactions in parallel, we can analyze the influence of the CH stretching vibration for both reactions at the same time.

RESULTS

We recorded the I^- product ions of the S_N2 reaction and CH_2I^- ions resulting from the proton transfer reaction with a velocity map imaging spectrometer. Angle and energy differential scattering cross sections are obtained for both product ions, alternating with and without the vibrational excitation laser present, as detailed in the Materials and Methods section. For the reactants, a relative collision energy of 0.71 eV is chosen, which is slightly smaller than the energy necessary to promote the proton transfer channel, as this starts to appear at a collision energy of approximately 0.8 eV (*31*). Excitation of one quantum in the CH symmetric stretch (near 2971 cm^{-1} or 0.37 eV) is sufficient to overcome the threshold for proton transfer. The difference signal between the scattering experiments with infrared (IR_{on}) and without IR excitation (IR_{off}) provides a direct measure of the effect vibrational excitation has on the reaction rate. The simultaneous recording of both reaction channels allows a direct comparison of the intensities of I^- and CH_2I^- product ions with and without the vibrational excitation laser present.

Figure 2 shows time-of-flight traces for the relative collision energy of 0.71 eV with and without IR excitation compared with a trace for a collision energy of 1.17 eV, where the proton transfer channel is energetically open. Table 1 presents the number of counts for both channels

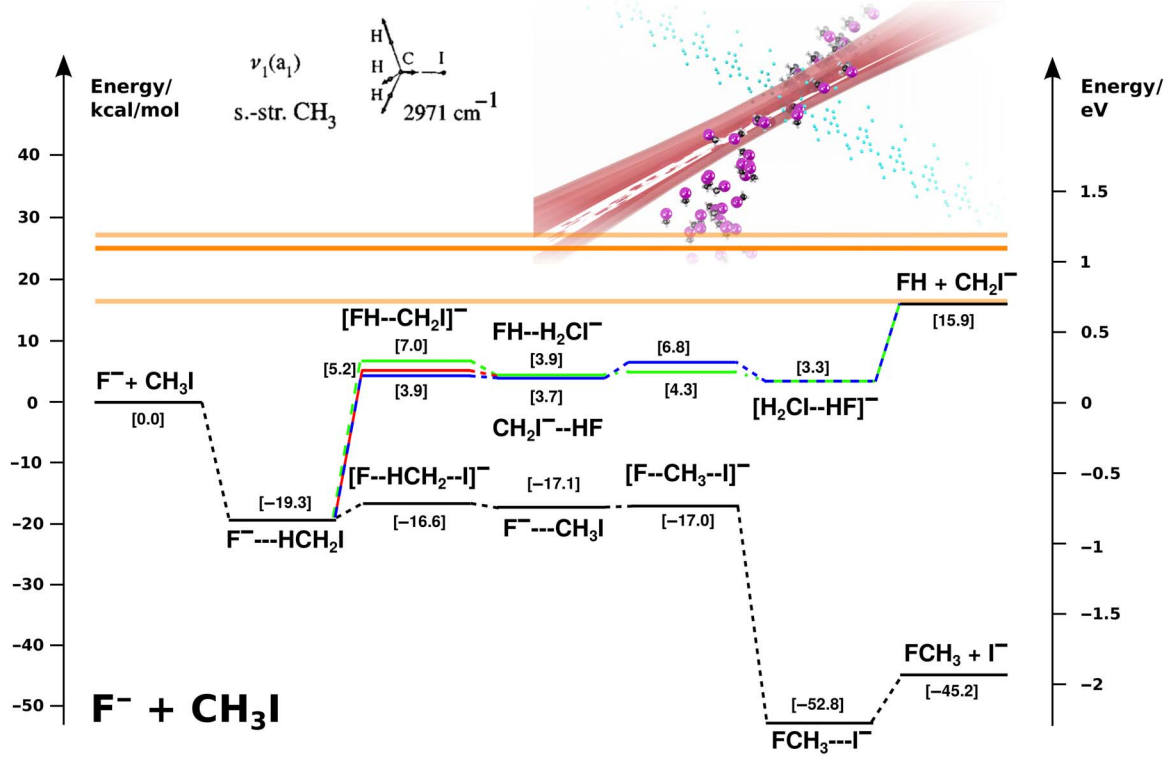

Fig. 1. Stationary points along the reaction coordinate of the reaction F^- + CH_3I for the S_N2 and the proton transfer reaction channel [taken from (*33*)]. Both reaction channels proceed via the same pre-reaction complex, in which the fluoride anion is hydrogen-bonded to an H atom. The transition state of the S_N2 is submerged, whereas a barrier exists for the proton transfer. Intrinsic reaction coordinate computations find three interconnected proton transfer pathways. The $[FH--CH_2I]^-$ transition state of the most direct pathway, which is marked in green, is used for the SVP analysis. The relative translational collision energies are marked with the light orange lines, and the total translational and vibrational energy of the CH-stretch excited reactants is marked with the bright orange line. The inset shows a sketch of the scattering experiment with CH_3I excited in the symmetric (a_1) CH stretching mode at 2971 cm^{-1} or 0.37 eV.

and the difference signal, including the respective statistical counting errors. The total recorded counts of more than 7×10^5 show that the S_N2 channel is by far the dominant reaction channel. We found a relative enhancement of the count rate of 0.30 ± 0.23%, which is barely statistically significant. Although the total number of counts is significantly less in the proton transfer channel, its relative enhancement of 31 ± 5% is a hundred times that of the S_N2 reaction and much larger than the statistical accuracy. However, note that on an absolute scale, the enhancement of the product flux in the proton transfer channel is smaller than in the S_N2 channel. The proton transfer signal without infrared excitation, at a collision energy that is close to the threshold energy, is attributed to the high-energy tail of the collision energy distribution. To quantify the change in the reaction cross section, the fraction of vibrationally excited CH_3I molecules within the interaction region is a requirement. This excited fraction was determined to be 1.4 ± 0.5% by taking the spatial and temporal overlap of all three beams into account, that is, neutral beam, ion beam, and laser beam, as shown in Fig. 3 (see Materials and Methods below). For the S_N2 reaction, this leads to a measured increase of the reaction cross section due to vibrational excitation by 21 ± 16%, which is again barely statistically significant. For comparison, increasing the translational energy by an amount similar to the vibrational excitation leads to a slight reduction of the rate coefficient (*32*). Taking the excited fraction into account, the proton transfer reaction is enhanced by a factor of 22 ± 4, two orders of magnitude more than the S_N2 reaction, in line with the opening of this reaction for all vibrationally excited molecules.

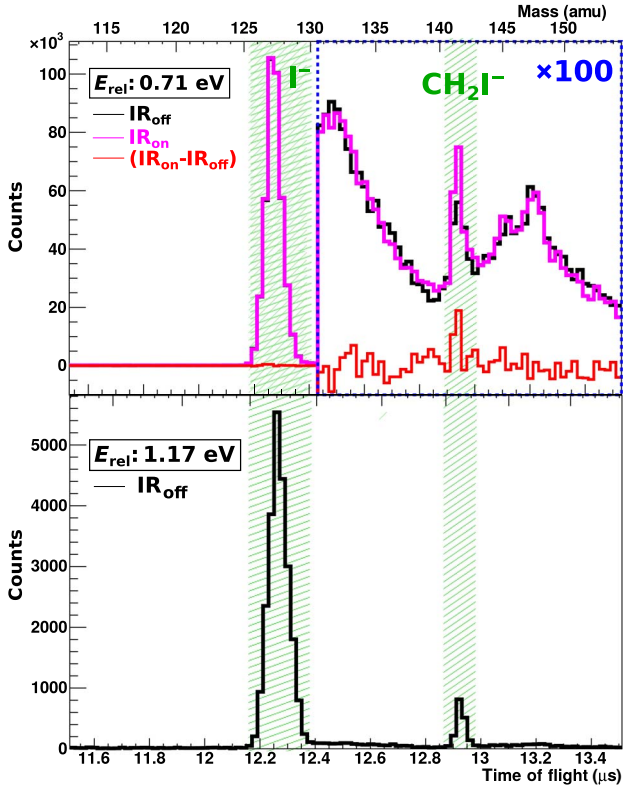

Fig. 2. Time-of-flight traces of the reaction products of the F^- + CH_3I reaction for two different relative collision energies. The conversion to atomic mass units (amu) is plotted on the upper horizontal axis. At the lower collision energy, we performed every other ion-molecule crossing with the infrared excitation laser present. The difference signal is plotted in red.

The experimental finding shows that the CH symmetric stretching mode acts as an almost complete spectator in the nucleophilic substitution reaction. To investigate this further, we performed QCT simulations on an ab initio–based full-dimensional PES (*33*) for reactions with methyl iodide in $\nu_1 = 0$ and 1 (see Materials and Methods section for details). We obtained total cross sections for the S_N2 reaction of 13.0 $Å^2$ for $\nu_1 = 0$ and 13.9 $Å^2$ for $\nu_1 = 1$ at the same collision energy of 0.71 eV, as in the experiment. This corresponds to a change in cross section due to vibrational excitation of only 6%, which agrees very well with the experimental observation that the CH symmetric stretching vibration acts as a spectator in this reaction. In the QCT simulation, we also find almost no difference for the reaction probability as a function of the impact parameter of the collision, which further strengthens the spectator character of the excited vibrational mode. For the proton transfer, our QCT calculations find an enhancement factor due to vibrational excitation of at least 4, with the result strongly depending on the treatment of the zero-point energy. Earlier QCT calculations for the reaction F^- + CH_3Cl also found that the cross section for proton transfer is significantly enhanced for CH vibrationally excited CH_3Cl compared to the reaction of ground-state molecules. There, the excitation of the CH symmetric stretch has a slightly larger effect on the S_N2 channel of about 10 to 30% increase, depending on collision energy (*29*). In contrast, for the S_N2 reaction Cl^- + CH_3Br, Hennig and Schmatz (*27*) questioned the spectator character of the symmetric CH stretching mode. In quantum dynamics calculations, they found that the influence of the CH symmetric stretch is not negligible but, instead, increases the cross section by more than one order of magnitude compared to the ground state and the introduction of the same energy in the form of translation. This result disagrees with our combined experimental and theoretical finding of spectator-like behavior of this vibrational mode in the present S_N2 reaction. We surmise that this is caused by the reduced dimensionality of the quantum scattering calculations, but further investigations are needed to clarify this.

We obtained more information on the dynamics of the vibrationally mediated proton transfer reaction from the differential scattering cross section measured for this reaction. Specifically, we extracted the differential scattering data from the difference of

Table 1. Product ion counts with and without vibrational excitation for the S_N2 and proton transfer reaction channels at a collision energy of 0.71 eV.

	Counts (IR_{on})	Counts (IR_{off})	(IR_{on}-IR_{off})	Rel. difference	Relative rate increase*
S_N2	389,726	388,552	1174 ± 882	(0.30 ± 0.23)%	0.21 ± 0.16
Proton transfer	1,191	911	280 ± 46	(31 ± 5)%	22 ± 4

*The rate increase is based on an excited fraction of (1.4 ±0.5)% (see the Materials and Methods section for details).

the CH_2I^- product ion velocity maps with and without vibrational excitation at a collision energy of 0.71 eV. These data are shown in Fig. 4 (top panels). We compare them to the scattering distribution of CH_2I^- ions from the reaction of ground-state CH_3I molecules at a collision energy of 1.17 eV, which corresponds to a similar total energy (bottom panels in Fig. 4). Besides the larger statistical fluctuations, the differential cross sections for the proton transfer reaction from vibrationally excited reactants agree fairly well with the data obtained for proton transfer that is activated by translational energy. Thus, adding energy in the form of vibration or translation does not change the dynamics of the proton transfer reaction. This is directly visible in the two-dimensional (2D) images in Fig. 4A and more quantitatively shown in the angular scattering and internal energy distributions (Fig. 4, B and C). The product ions are scattered predominantly isotropically with a slight propensity for direct forward and backward scattering. For the vibrational ground state, this agrees with previous experiments (*31*) and direct dynamics simulations (*35*). Our QCT simulations also reproduce the angular and energy distributions reasonably well, both for the ground and the excited vibrational state, as shown in Fig. 4 (B and C).

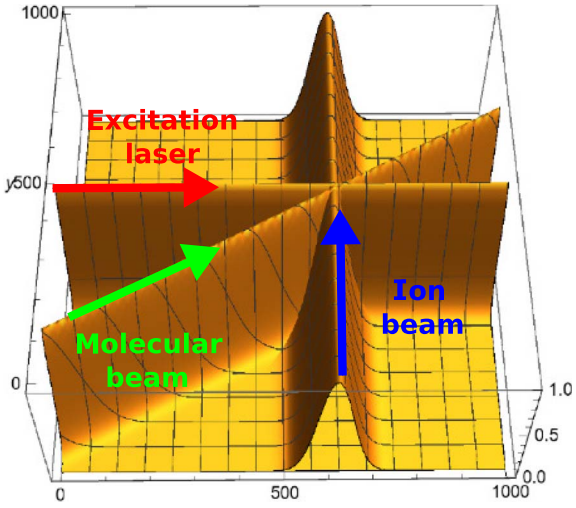

Fig. 3. Illustration of the overlap of the overlap of the molecular beam, ion beam, and laser beam and laser beams in the center of the velocity map imaging spectrometer. From the overlap integral, we determined the excited fraction of the neutral molecules in the reaction volume.

To better understand the influence of different reactant vibrational modes on the S_N2 and the proton transfer reactions, we applied the SVP model, a well-defined generalization of the classical Polanyi rules, to the present reactions (details are given in the Materials and Methods section). This allows us to compare the effect of adding translational or vibrational energy on the reaction cross section. The SVP model is only valid for direct reaction mechanisms; indirect channels with energy randomization in the entrance well would undercut its validity (*30*). However, at the present collision energy, the QCT simulations show that direct channels account for more than 50% of the reactivity. Table 2

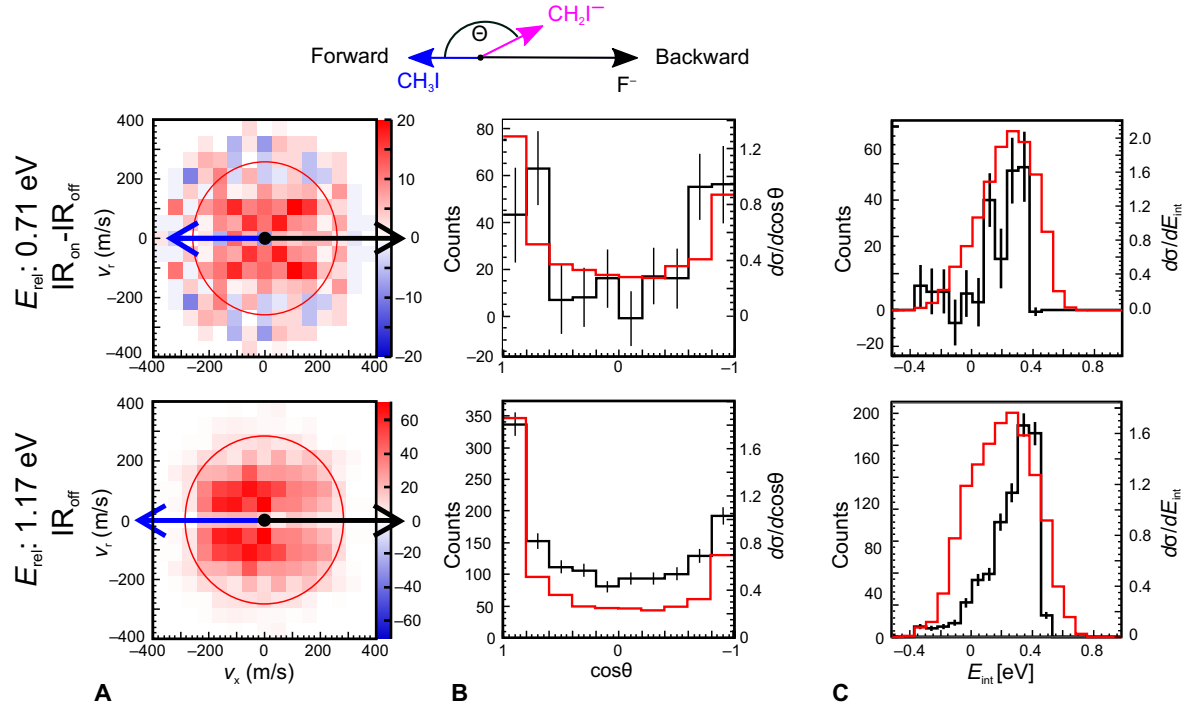

Fig. 4. Differential scattering data for the reaction $F^- + CH_3I \rightarrow CH_2I^- + HF$ for ground state and vibrationally excited CH_3I molecules compared to results from QCT simulations. (**A**) Center-of-mass angle and velocity differential cross sections for CH_2I^- ions at 0.71 eV (top) and 1.17 eV (bottom) collision energy. We obtained the distributions at 0.71 eV collision energy by subtracting the contribution of ground-state reactions from the signal for reactions obtained with CH_3I ($v_1 = 1$) vibrationally excited molecules. The red circle indicates the kinematic cutoff. Relative orientations of the velocity vectors are indicated in the Newton diagram. (**B**) Measured (black line) and simulated (red line) angular distributions are shown for vibrationally excited and ground-state reactants. Both velocity integrated angular distributions show an isotropic component and a small amount of forward and backward scattering. (**C**) Measured internal energy distributions (black line) for the product species are in good overall agreement with the QCT simulations (red line). The internal energy is expected to be locked up in CH_2I^-, as previous simulations already showed that HF acquired almost no internal excitation (*35*). We found a similar degree of internal excitation for CH_2I^- for experiments with and without IR excitation.

Table 2. SVP values for normal modes of CH_3I projected onto the reaction coordinates at transition states for the proton transfer and the nucleophilic substitution channel.

	Proton transfer	Nucleophilic substitution
CI stretch	0.22	0.78
CH_3 rocking	0.09	0.00
CH_3 umbrella	0.76	0.24
CH_3 deformation	0.30	0.00
CH symmetric stretch	0.33	0.03
CH asymmetric stretch	0.10	0.00
Translation	0.02	0.16

shows the SVP values for S_N2 reactions via backside attack of the nucleophile. We find a rather small value for the CH symmetric stretching mode, more than five times smaller than the value for adding translational energy. This is consistent with the relatively inefficient coupling of the vibrational mode to the reaction coordinate at the transition state and thus the general spectator mode behavior of the symmetric CH stretch. The SVP analysis shows that the most effective form of promoting the S_N2 reaction will be the excitation of the CI stretching vibration. Our QCT calculations support this finding, but previous experiments disagree with this (*32*). For the direct proton transfer pathway (see Fig. 1), the SVP analysis found the CH symmetric stretching vibration to have a strong coupling with the reaction coordinate at the transition state (see Table 2).

DISCUSSION

The observed ineffectiveness of the excitation of the CH symmetric stretching vibration provides direct experimental proof of the spectator mode character of this vibration for the nucleophilic substitution reaction. Our combined experimental and computational work demonstrates that probing of mode-specific dynamics is possible in polyatomic physical organic chemistry reactions, where the SVP model provides a powerful generalization of the Polanyi rules. In the future, the reaction dynamics following vibrational excitation in the very interesting lower-frequency umbrella and CI stretching modes will also become accessible. Our results also pave the way for studies on the mode-selective control of the branching into very different reaction mechanisms in polyatomic reactions. It will be particularly interesting to investigate vibrational control of the competing nucleophilic substitution and elimination reactions that have been disentangled recently (*36*).

MATERIALS AND METHODS

Crossed-beam ion imaging

A detailed description of the experimental setup and the data analysis was published before (*22*, *37*), and only a brief description of the experimental procedures is given here. An ion beam of fluoride anions was produced by a pulsed plasma discharge of NF_3 seeded in argon. The F^- ions were mass-selected and transferred into a radio frequency octopule ion trap where they thermalized in a buffer gas at room temperature. Ion extraction was adjusted to yield energy distributions with a tunable kinetic energy and a typical full width at half maximum (FWHM) of below 200 to 250 meV. In the center of the velocity map imaging spectrometer, the ions were crossed at 60° with a supersonic molecular beam of methyl iodide molecules seeded in argon (~10% CH_3I/Ar). In the center-of-mass frame of reference, the collision kinematics led to a spread of the relative collision energy of below 170 meV FWHM. I^- product ions were extracted normal to the scattering plane and mapped onto a position and time-sensitive detector. Simultaneous recording of the 2D position vector on the detector and the time of flight of the product ions enabled us to determine the 3D velocity vector and the branching into competing reaction product channels (*38*).

Reactant vibrational excitation

At the collision energy of 0.71 eV, reactive scattering events were alternately recorded with either all CH_3I molecules in the vibrational ground state or with a fraction of the molecules in the $v_1 = 1$ vibrationally excited state. Vibrational excitation was provided before scattering by IR laser pulses (0.2 mJ per pulse) at a frequency of 2971 cm^{-1} (0.37 eV) produced by difference frequency mixing of the light of a pulsed dye laser (Radiant Dyes) with a seeded Nd:YAG laser (Innolas). The crossed-beam imaging experiment was operated at a repetition rate of 20 Hz. The infrared laser pulses with a repetition rate of 10 Hz were synchronized such that every other ion-molecule crossing occurs with and without infrared excitation, respectively. The obtained time-of-flight spectra at 0.71 eV collision energy are presented in Fig. 2, together with a time-of-flight trace at the higher collision energy of 1.17 eV. Counting the number of events in the shaded regions yields the data presented in Table 1.

The fraction of excited molecules was probed by a scheme adapted from Hu *et al.* (*39*). At first, the infrared excitation pulse was passed through the molecular beam entrained with CH_3I. Then, CH_3I was photodissociated with 266 nm laser pulses, and the CH_3 fragments were subsequently ionized by 2 + 1 resonance-enhanced multiphoton ionization, selectively addressing fragments in the vibrational ground state. Vibrational excitation of CH_3I leads to depletion of the ground-state CH_3 fragment signal, since the CH stretching vibrational excitation is preserved in the fragment. From the difference in count rate, a depletion value of 2.0 ± 0.2% was determined, which amounted to the fraction of excited CH_3I molecules in the interaction volume of the detection lasers.

The interaction volume of molecular and ion beam further limits the fraction of excited CH_3I molecules that can possibly react with the fluoride anions. Thus, the temporal and the spatial overlap of all three beams involved should be considered. The temporal propagation of the excited molecules was taken into account by a delay between excitation and extraction. The determination of the spatial overlap requires knowledge of the positions of each beam. We performed an analysis of the spatial distribution of the ion beam. The position of the beam can be projected onto the detector using spatial map imaging (*40*). The mean position and the extension perpendicular to the propagation directions were approximated by a Gaussian distribution. Cylindrical symmetry of the beam was assumed due to last lenses within the beam path being cylindrical. The vertical dimension of the neutral beam was determined by scanning the laser through the beam. Again, cylindrical symmetry was assumed. The position of the beam was probed by spatial mapping of the CH_3I^+ cations produced by laser ionization. The size of the laser beam was measured by blocking the beam with a movable razor blade and recording the transmitted power. The relative overlap of all three beams was then determined from the 3D overlap integral of the beams

(see Fig. 3). The ratio between the overlaps amounted to 0.65. Thus, on average, 65% of the CH_3I molecules interacting with the ion beam were excited to the mean excited fraction. This gave an effective mean excited fraction of 1.4 ± 0.5% in the interaction region of the crossed beams.

Intramolecular vibrational energy redistribution of the infrared excitation in the fundamental CH stretching vibration was not expected to be important, since its frequency does not overlap with harmonics of the lower vibrational modes. We verified this experimentally by measuring the excited state fraction for different delays between the excitation pulse and the detection pulses up to several microseconds, and we did not detect any changes in the excited-state fraction.

Dynamics simulations

QCT computations were performed at collision energies of 0.71 and 1.17 eV for the $F^- + CH_3I$ (v_1 = 0,1) reactions using a global, ab initio, analytical, full-dimensional PES (*33*), which describes both the S_N2 and proton transfer channels. The initial ground and symmetric CH stretching excited vibrational state were prepared using standard normal mode sampling. The rotational angular momentum (rotational temperature) of CH_3I was set to zero by initial velocity adjustments. The relative orientations of the reactants were randomly sampled, and the initial distances were $(x^2 + b^2)^{1/2}$, where b is the impact parameter and x is set to 20 bohr (10.6 Å). b was scanned from 0 to b_{max} with steps of 0.5 bohr, where the b_{max} values were 13.0 bohr at 0.71 eV and 11.0/11.5 bohr at 1.17 eV for v_1 = 0/1. Five thousand trajectories were computed at each b; thus, this study considered roughly half a million trajectories. Integral and differential cross sections were obtained by a b-weighted numerical integration of the reaction probabilities over impact parameters.

Sudden Vector Projection model

The SVP model (*12*) is based on the premise that the ability of a reactant mode in promoting the reaction is proportional to its coupling with the reaction coordinate at a transition state. This correlation is reasonable for direct reactions in which the collision time is significantly shorter than that needed for intramolecular vibrational energy redistribution of the reactants. This model can be considered as a generalization of the Polanyi rules for atom-diatom reactions (*1*), which attribute the relative efficacies of the reactant vibrational and translational excitations to the location of the transition state. The SVP model was successfully demonstrated in a large number of reactions (*41*), including the $F^- + CH_3Cl$ S_N2 reaction (*30*).

The SVP model was applied here to rationalize the mode specificity in both the S_N2 and proton transfer reactions. In the S_N2 reaction, we focused on the backside attack transition state as the frontside attack represents a minor channel. For the proton transfer reaction, we concentrated on the primary transition state, which is also involved in the double-inversion pathway (*33*, *42*). This was based on the fact that this transition state is directly involved in the cleavage of the CH bond, whereas the other pathways involve much more complex intrinsic reaction coordinates. The SVP values for the proton transfer transition state are collected in Table 2, along with those for the Walden inversion transition state.

REFERENCES AND NOTES

1. J. C. Polanyi, Some concepts in reaction dynamics. *Acc. Chem. Res.* **236**, 680–690 (1972).
2. R. N. Zare, Laser control of chemical reactions. *Science* **279**, 1875–1879 (1998).
3. F. F. Crim, Chemical dynamics of vibrationally excited molecules: Controlling reactions in gases and on surfaces. *Proc. Natl. Acad. Sci. U.S.A.* **105**, 12654–12661 (2008).
4. W. Zhang, H. Kawamata, K. Liu, CH stretching excitation in the early barrier F + CHD_3 reaction inhibits CH bond cleavage. *Science* **325**, 303–306 (2009).
5. F. Wang, K. Liu, Enlarging the reactive cone of acceptance by exciting the C–H bond in the $O(^3P)$ + CHD_3 reaction. *Chem. Sci.* **1**, 126–133 (2010).
6. T. Wang, J. Chen, T. Yang, C. Xiao, Z. Sun, L. Huang, D. Dai, X. Yang, D. H. Zhang, Dynamical resonances accessible only by reagent vibrational excitation in the F + HD → HF + D reaction. *Science* **342**, 1499–1502 (2013).
7. R. Liu, F. Wang, B. Jiang, G. Czakó, M. Yang, K. Liu, H. Guo, Rotational mode specificity in the Cl + CHD_3 → HCl + CD_3 reaction. *J. Chem. Phys.* **141**, 074310 (2014).
8. H. Hou, Y. Huang, S. J. Gulding, C. T. Rettner, D. J. Auerbach, A. M. Wodtke, Enhanced reactivity of highly vibrationally excited molecules on metal surfaces. *Science* **284**, 1647–1650 (1999).
9. R. D. Beck, P. Maroni, D. C. Papageorgopoulos, T. T. Dang, M. P. Schmid, T. R. Rizzo, Vibrational mode-specific reaction of methane on a nickel surface. *Science* **302**, 98–100 (2003).
10. J. Liu, S. L. Anderson, Dynamical control of 'statistical' ion–molecule reactions. *Int. J. Mass Spectrom.* **241**, 173–184 (2005).
11. F. Wang, J.-S. Lin, K. Liu, Steric control of the reaction of CH stretch–excited CHD_3 with chlorine atom. *Science* **331**, 900–903 (2011).
12. B. Jiang, H. Guo, Relative efficacy of vibrational vs. translational excitation in promoting atom-diatom reactivity: Rigorous examination of Polanyi's rules and proposition of sudden vector projection (SVP) model. *J. Chem. Phys.* **138**, 234104 (2013).
13. K. P. C. Vollhardt, N. E. Shore, *Organic Chemistry, Structure and Function* (Pallgrave Macmillan, 2007).
14. W. N. Olmstead, J. I. Brauman, Gas-phase nucleophilic displacement reactions. *J. Am. Chem. Soc.* **99**, 4219–4228 (1977).
15. P. Manikandan, J. Zhang, W. L. Hase, Chemical dynamics simulations of $X^- + CH_3Y \rightarrow XCH_3 + Y^-$ gas-phase S_N2 nucleophilic substitution reactions. nonstatistical dynamics and nontraditional reaction mechanisms. *J. Phys. Chem. A* **116**, 3061–3080 (2012).
16. S. Liu, H. Hu, L. G. Pedersen, Steric, quantum, and electrostatic effects on S_N2 reaction barriers in gas phase. *J. Phys. Chem. A* **114**, 5913–5918 (2010).
17. A. A. Viggiano, R. A. Morris, J. S. Paschkewitz, J. F. Paulson, Kinetics of the gas-phase reactions of chloride anion, Cl^- with CH_3Br and CD_3Br: experimental evidence for nonstatistical behavior? *J. Am. Chem. Soc.* **114**, 10477–10482 (1992).
18. V. F. DeTuri, P. A. Hintz, K. M. Ervin, Translational activation of the S_N2 nucleophilic displacement reactions $Cl^- + CH_3Cl$ (CD_3Cl) → $ClCH_3$ ($ClCD_3$) + Cl^-: A guided ion beam study. *J. Phys. Chem. A* **101**, 5969–5986 (1997).
19. J. Mikosch, S. Trippel, C. Eichhorn, R. Otto, U. Lourderaj, J. X. Zhang, W. L. Hase, M. Weidemüller, R. Wester, Imaging nucleophilic substitution dynamics. *Science* **319**, 183–186 (2008).
20. J. Xie, R. Otto, J. Mikosch, J. Zhang, R. Wester, W. L. Hase, Identification of atomic-level mechanisms for gas-phase $X^- + CH_3Y$ S_N2 reactions by combined experiments and simulations. *Acc. Chem. Res.* **47**, 2960–2969 (2014).
21. M. Stei, E. Carrascosa, M. A. Kainz, A. H. Kelkar, J. Meyer, I. Szabó, G. Czakó, R. Wester, Impact of the leaving group on the dynamics of a gas phase S_N2 reaction. *Nat. Chem.* **8**, 151–156 (2016).
22. J. Mikosch, J. Zhang, S. Trippel, C. Eichhorn, R. Otto, R. Sun, W. A. de Jong, M. Weidemüller, W. L. Hase, R. Wester, Indirect dynamics in a highly exoergic substitution reaction. *J. Am. Chem. Soc.* **135**, 4250–4259 (2013).
23. S. R. Vande Linde, W. L. Hase, A direct mechanism for S_N2 nucleophilic substitution enhanced by mode selective vibrational excitation. *J. Am. Chem. Soc.* **111**, 2349–2351 (1989).
24. W. L. Hase, Simulations of gas-phase chemical reactions: Applications to S_N2 nucleophilic substitution. *Science* **266**, 998–1002 (1994).
25. P. Ayotte, J. Kim, J. A. Kelley, S. B. Nielsen, M. A. Johnson, Photoactivation of the $Cl^- + CH_3Br$ S_N2 reaction via rotationally resolved C-H stretch excitation of the Cl^-·CH_3Br entrance channel complex. *J. Am. Chem. Soc.* **121**, 6950–6951 (1999).
26. D. S. Tonner, T. B. McMahon, Non-statistical effects in the gas phase S_N2 reaction. *J. Am. Chem. Soc.* **122**, 8783–8784 (2000).
27. C. Hennig, S. Schmatz, Spectator modes in reaction dynamics revisited: Reaction cross sections and rate constant for $Cl^- + CH_3Br \rightarrow ClCH_3 + Br^-$ from quantum scattering. *Chem. Phys. Lett.* **446**, 250–255 (2007).
28. M. Kowalewski, J. Mikosch, R. Wester, R. de Vivie-Riedle, Nucleophilic substitution dynamics: Comparing wave packet calculations with experiment. *J. Phys. Chem. A* **118**, 4661–4669 (2014).
29. I. Szabó, G. Czakó, Revealing a double-inversion mechanism for the F^-+CH_3Cl S_N2 reaction. *Nat. Commun.* **6**, 5972 (2015).
30. Y. Wang, H. Song, I. Szabó, G. Czakó, H. Guo, M. Yang, Mode-specific S_N2 reaction dynamics. *J. Phys. Chem. Lett.* **7**, 3322–3327 (2016).

31. E. Carrascosa, T. Michaelsen, M. Stei, B. Bastian, J. Meyer, J. Mikosch, R. Wester, Imaging proton transfer and dihalide formation pathways in reactions of F^- + CH_3I. *J. Phys. Chem. A* **120**, 4711–4719 (2016).
32. T. Su, R. A. Morris, A. A. Viggiano, J. F. Paulson, Kinetic energy and temperature dependences for the reactions of fluoride with halogenated methanes: Experiment and theory. *J. Phys. Chem.* **94**, 8426–8430 (1990).
33. B. Olasz, I. Szabó, G. Czakó, High-level *ab initio* potential energy surface and dynamics of the F^- + CH_3I S_N2 and proton-transfer reactions. *Chem. Sci.* **8**, 3164–3170 (2017).
34. D. M. Bell, S. L. Anderson, Vibrationally enhanced charge transfer and mode/bond-specific H^+ and D^+ transfer in the reaction of HOD^+ with N_2O. *J. Chem. Phys.* **139**, 114305 (2013).
35. J. Zhang, J. Xie, W. L. Hase, Dynamics of the F^- + CH_3I → HF + CH_2I^- proton transfer reaction. *J. Phys. Chem. A* **119**, 12517–12525 (2015).
36. E. Carrascosa, J. Meyer, J. Zhang, M. Stei, T. Michaelsen, W. L. Hase, L. Yang, R. Wester, Imaging dynamic fingerprints of competing E2 and S_N2 reactions. *Nat. Commun.* **8**, 25 (2017).
37. R. Wester, Velocity map imaging of ion–molecule reactions. *Phys. Chem. Chem. Phys.* **16**, 396–405 (2014).
38. S. Trippel, M. Stei, R. Otto, P. Hlavenka, J. Mikosch, C. Eichhorn, A. Lourderaj, J. X. Zhang, W. L. Hase, M. Weidemüller, R. Wester, Kinematically complete chemical reaction dynamics. *J. Phys. Conf. Ser.* **194**, 012046 (2009).
39. L. Hu, Z. Zhou, C. Dong, L. Zhang, Y. Du, M. Cheng, Q. Zhu, Vibrationally mediated photodissociation of CH_3I [v_1 = 1] at 277.5 nm: The vibrationally adiabatic process. *J. Phys. Chem. A* **117**, 4352–4357 (2013).
40. M. Stei, J. von Vangerow, R. Otto, A. H. Kelkar, E. Carrascosa, T. Best, R. Wester, High resolution spatial map imaging of a gaseous target. *J. Chem. Phys.* **138**, 214201 (2013).
41. H. Guo, B. Jiang, The sudden vector projection model for reactivity: Mode specificity and bond selectivity made simple. *Acc. Chem. Res.* **47**, 3679–3685 (2014).
42. Y.-T. Ma, X. Ma, A. Li, H. Guo, L. Yang, J. Zhang, W. L. Hase, Potential energy surface stationary points and dynamics of the F^- + CH_3I double inversion mechanism. *Phys. Chem. Chem. Phys.* **19**, 20127–20136 (2017).

Acknowledgments

Funding: This work is supported by the Austrian Science Fund (FWF) (project P 25956-N20). E.C. acknowledges the support from DOC Fellowship by the Austrian Academy of Sciences (ÖAW). G.C. thanks the Scientific Research Fund of Hungary (PD-111900 and K-125317) for the financial support and the National Information Infrastructure Development Institute for computer resources. A.L. acknowledges the National Natural Science Foundation of China (21203259), and H. G. acknowledges a grant from the Air Force Office of Scientific Research (FA9550-15-1-0305). **Author contributions:** M.S., A.D., E.C., and J.M carried out the experiment. M.S. analyzed the data. B.O. and G.C. carried out the trajectory simulations. A.L. and H.G. performed the SVP analysis. R.W. conceived the experiment and supervised the project. M.S., J.M., and R.W. wrote the manuscript. **Competing interests:** The authors declare that they have no competing interests. **Data and materials availability:** All data needed to evaluate the conclusions in the paper are present in the paper. Additional data related to this paper may be requested from the authors.

Submitted 9 January 2018
Accepted 22 May 2018
Published 6 July 2018
10.1126/sciadv.aas9544

Citation: M. Stei, E. Carrascosa, A. Dörfler, J. Meyer, B. Olasz, G. Czakó, A. Li, H. Guo, R. Wester, Stretching vibration is a spectator in nucleophilic substitution. *Sci. Adv.* **4**, eaas9544 (2018).